Geoderma 317 (2018) 23–31

Contents lists available at ScienceDirect

Geoderma

journal homepage: www.elsevier.com/locate/geoderma

Detecting nonlinearity in the spatial series of nitrous oxide emission by delay vector variance

Wenxiu Zou[a,1], Wenjun Ji[b,1], Bing Cheng Si[c], Asim Biswas[d,*]

[a] Northeast Institute of Geography and Agroecology, Chinese Academy of Sciences, No.138 Haping Road, Harbin, 150081 China
[b] Department of Bioresource Engineering, McGill University, 21111 Lakeshore Road, Ste-Anne-de-Bellevue, QC H9X 2V9, Canada
[c] Department of Soil Science, University of Saskatchewan, 51 Campus Drive, Saskatoon, SK S7N 5A8, Canada
[d] School of Environmental Sciences, University of Guelph, 50 Stone Road East, Guelph, ON N1G 2W1, Canada

ARTICLE INFO

Handling Editor: A.B. McBratney

Keywords:
Nonlinearity
Data analysis
Spatial and temporal variability
Greenhouse gas
Climate change

ABSTRACT

Soil spatial variability may exhibit nonlinearity and this has been assumed in studies without proper quantification. Owing to the complexity of underlying biogeochemical processes, greenhouse gas emission, in particular, nitrous oxide (N_2O) flux from soil, is highly variable over space and time. The goal of this work was to examine the nonlinearity associated with the spatial series of N_2O flux from soil using the delay vector variance (DVV) method. DVV uses the predictability of a spatial series in a phase-space to identify linearity/nonlinearity within a data series using a surrogate data methodology to derive a test statistic. A two-piece closed vented chamber was used to measure N_2O fluxes along a transect of 128 points located within the hummocky landscape of central Saskatchewan, Canada. There was nonlinearity associated with the spatial series of early spring and spring measurements. The uneven distribution of snowmelt water facilitated the favourable situations for denitrifying bacterial activity creating hotspots for denitrification processes. The flux measured during the fall season exhibited a nonlinear pattern, whereas the flux measured during the time of plant growth exhibited a linear pattern over space. Strong evapotranspiration demand during the growing season in the semi-arid climate of the study area controlled the hydrological processes and thus, the spatial N_2O flux measurements giving rise to a linear spatial pattern. The DVV detected nonlinearity in a spatial series will improve the understanding of the complexity of underlying soil processes.

1. Introduction

Soil spatial variability is inescapable and influences the precision of any statement that can be made about soil properties at any location (Trangmar et al., 1985). Information about soil spatial variability is necessary for enhanced agricultural and environmental management (Trangmar et al., 1985), soil quality assessment (Heuvelink and Pebesma, 1999), soil-landscape process modelling (Corwin et al., 2006), and natural resource management. Systematic studies have identified various aspects of soil spatial variability including spatial autocorrelations or dependence (Trangmar et al., 1985), periodic or cyclical patterns (Kachanoski et al., 1985), and nonstationarity (Biswas and Si, 2011; Biswas and Si, 2013; Lark et al., 2004b). Additionally, the variability of a soil property cannot be quantified by observing the effect from each factor individually and adding them subsequently. For example, soil water storage that can directly regulate the gas flux from soil may be controlled by a series of environmental factors and processes such as topography, vegetation, and rainfall. The combined influences of these factors may not be the same as the sum of the individual influences. Therefore, the processes determining variation in a soil spatial series cannot be represented using a linear function or equation (Biswas et al., 2013; Pai and Palazotto, 2008). In this situation, the spatial series may exhibit nonlinearity because of the nonlinear responses from underlying soil processes. While other fields of science may define nonlinearity differently (Emanuel, 1997; Jaksic et al., 2016; Mandic et al., 2008; Schreiber, 1999), in this manuscript, we refer to the outcome of nonlinear responses from underlying soil processes on the spatial series of soil measurements.

Geostatistical, spectral and wavelet analyses have been used for characterizing, simulating and interpolating spatial series in soils. However, all these methods assume the data series of soil properties created by the underlying soil processes that can be represented by a linear function. The variability of soil properties is controlled by numerous environmental factors and processes that may affect soil

* Corresponding author.
E-mail addresses: wxzou_540@163.com (W. Zou), wenjun.ji@mail.mcgill.ca (W. Ji), bing.si@usask.ca (B.C. Si), biswas@uoguelph.ca (A. Biswas).
[1] Contribution equally shared between two first authors.

https://doi.org/10.1016/j.geoderma.2017.12.023
Received 17 September 2017; Received in revised form 8 November 2017; Accepted 20 December 2017
Available online 30 December 2017

individually, or in combination. Therefore, the spatial series of soil properties resulting from these complex interactions and their variability may cause a spatial series, that may not be represented by a linear function (Biswas et al., 2013). Even though the soil system is fundamentally deterministic (variations in soil properties are caused by the underlying processes and they are not random), it may exhibit some degree of randomness. The randomness may arise from the underlying strong variability of environmental factors and processes and may not show any predictable behaviour over space. Therefore, nonlinearity is one of the important aspects associated with a spatial series and needs to be examined for quantifying soil spatial variation.

Nonlinear Dynamical System Theory (Fuchs, 2013) has been used to explain the long-term quantitative behaviour of dynamical systems such as physical and biological. It studies the nature and workable solutions of phenomena that is variable over time and often mechanical and physical in nature. It concentrates more on understanding the system's behaviour over time than determining the actual solutions of the causes that have been used to explain and/or predict nonlinear evolution of soil formation (Phillips, 1998), ecological data (Turchin and Taylor, 1992) or complex soil systems (Culling, 1988). Similar to others methods, such as the spectral analysis, this time series based method (Nonlinear Dynamical System Theory) can be extended to study complex spatial soil systems (Millan et al., 2009). The variability of a spatial series where soil properties are measured as a function of spatial positions along a given direction, could be associated with a nonlinear response of many interacting variables and expressed as a stochastic or a deterministic function of measurement locations (Millan et al., 2009; Phillips, 1998; Phillips, 2008). However, unlike temporal measurements, there will be fewer variables that can be measured within a narrow range of spatial scales to analyze soil as a complex physical system. Therefore, alternative methods are required to quantify the spatial variability of soil properties with limited length of a spatial series.

Comparing several established nonlinearity analysis methods including deterministic versus stochastic plots (DVS) (Casdagli, 1992) and traditional nonlinearity matrices (Schreiber and Schmitz, 1997), such as third order autocovariance, time reversibility-based measure of deviation and δ-ε method (Kaplan, 1994), Gautama et al. (2004) introduced the delay vector variance (DVV) in detecting determinism and nonlinearity. The DVV assesses a series than a system as nonlinear and can be connected as the variations of a soil spatial series is the representation of underlying soil and environmental processes (Si, 2008). It characterizes a series based on its predictability and compares those obtained from linearized version of the series, i.e. surrogate data. The surrogate series are generated from the original series after destroying the underlying pattern. Thus, a comparison of DVVs between the unknown original series and the linearized version of the original series or surrogates may reveal the presence or absence of nonlinearity. Basically, it verifies if the series was generated by a linear stochastic system (Jaksic et al., 2016) or in the context of this manuscript, if the soil spatial series are generated by the linear response of underlying soil processes. It tests a series' deterministic-stochastic and linear-nonlinear behaviour simultaneously (Mandic et al., 2008). It is robust even in the presence of noise, straight forward to interpret and visualize, and does not require any prior knowledge of the series yet shows superior performance over other available methods (Gautama et al., 2004). It has been successfully used in many fields, including biomedical and health sciences (Mandic et al., 2008), mechanical engineering (Schreiber, 1999), construction engineering (Jaksic et al., 2015) and others mainly as time series analysis methods but shows strong promise to characterize nonlinear soil spatial variability.

Nitrous oxide (N_2O) is an important greenhouse gas contributing about 5% of the increased greenhouse effect (IPCC, 2007). Agriculture is one of the major sources of N_2O emissions contributing up to 84% of the global anthropogenic N_2O emissions (IPCC, 2007) and up to 70% of Canadian anthropogenic N_2O emissions (Environment Canada, 2008). N_2O emissions from agricultural soils are typically intermittent across the landscape and exhibit strong spatio-temporal variability in a complex way (Lark et al., 2004a; Lark et al., 2004b; Nieder and Benbi, 2008; Yates et al., 2006) and the emission rate is scale dependent (Milne et al., 2011; Milne et al., 2013; Yates et al., 2007). The processes that make the emission transient includes both denitrification and nitrification, although the former is generally more important. As the supply of the substrate to the denitrifying bacteria is limited to the micro sites, the control of denitrification is marked by nonlinear processes (Lark et al., 2004a; Lark et al., 2004b; Webster and Goulding, 1989). The water filled pore space (WFPS), as controlled by soil water content, is often determined in part by topography (Groffman and Tiedje, 1989), and is considered as the primary environmental factor controlling N_2O emissions from soil (Tian et al., 2015). Another key physical factor is soil temperature that determines the activity of soil microorganisms and controls N_2O emission (Creze, 2015).

The spatial variability of N_2O emissions from soil has been studied using advanced analysis techniques including wavelets (Lark et al., 2004a; Lark et al., 2004b; Milne et al., 2011; Milne et al., 2013; Yates et al., 2006; Yates et al., 2007). These studies used wavelet analysis to examine the spatial variability of N_2O emission that exhibited non-stationarity in the spatial series. Similarly, a spatial series can also exhibit nonlinear behaviour due to the nature of underlying soil processes (Anthony et al., 1995; Kroon et al., 2008; McSwiney and Robertson, 2005; Shcherbak et al., 2014) and thus, needs to be analyzed or examined. Therefore, the objective of this manuscript was to examine if the spatial series of N_2O emissions from soil exhibit nonlinearity using the delay vector variance. This will provide a framework for examining the presence or absence of nonlinearity in a spatial series of soil properties and can be used elsewhere.

2. Theory

The Delay Vector Variance (DVV) method characterizes a spatial series based upon its predictability and compares the results to those obtained for linearized versions of the series that are known as surrogates. The success of this method depends on two steps; 1) generation of the surrogate series, and 2) the test of nonlinearity.

2.1. Surrogate series generation

The nonlinearity analysis was performed by computing a test statistic for the original series based on 99 surrogates (this allowed for a one tailed statistical rank test at the level of 0.01). Surrogates are the realization of a composite null hypothesis and are generated from the linear and stationary processes driven by a Gaussian white noise input. The output of surrogates is the amplitude transformed by a zero-memory observation function (Gautama et al., 2004). Among the available methods for generating surrogate series (Schreiber and Schmitz, 2000), a well known is Iterative Amplitude Adjusted Fourier Transform (IAAFT), which is derived from the Amplitude Adjusted Fourier Transform (AAFT) (Theiler et al., 1992). The surrogates generated using IAAFT maintains the probability density functions and the power spectrum of the original series was used in this study. The surrogates were generated following the steps outlined below (Schreiber and Schmitz, 1996).

i. The spatial series$\{s_n\}$, $n = 1, \ldots, N$ was rank ordered according to a set of Gaussian random numbers. The sorted series $s_n' = g(s_n)$, followed the same spatial distribution as the original series, $\{s_n\}$ but Gaussian.
ii. The surrogates of $\{s_n'\}$ were phase randomized and marked them $\{\tilde{s}_n'\}$.
iii. The rescaling g was inverted by rank ordering $\{\tilde{s}_n'\}$ according to the distribution of the original series, $\{\tilde{s}_n = \overline{g}(\tilde{s}_n')\}$.
iv. Amplitudes of the Fourier transform of the sorted series $\{S_n\}$, were

squared, $|S_k|^2 = |\Sigma_{n=0}^{N-1} s_n e^{i2\pi kn/N}|^2$.

v. The original series, $\{s_n\}$ was shuffled (without replacement) randomly to destroy any nonlinear relationship without changing the probability density function. The shuffled series was the starting point of the iteration$\{s_n^{(0)}\}$ and each iteration consisted of the two following steps;
   a. For i^{th} iteration, the desired sample power spectrum of $\{s_n^{(i)}\}$, was calculated by taking the Fourier transform of $\{s_n^{(i)}\}$, and replacing the squared amplitude $\{s_k^{2,(i)}\}$ by $\{s_k^2\}$. By keeping the phases of the complex Fourier components unchanged, the inverse Fourier transform provided the same spectrum with a different probability distribution.
   b. The resulting series was then rank ordered and replaced each value with the values in the original series$\{s_n\}$. The replacement or the amplitude adaptation produced an updated series $\{S_n^{(i+1)}\}$.

vi. The Step v was repeated several times until the discrepancy in the power spectrum was below a threshold or the sequence stopped changing.

As the convergence of the iteration scheme was a function of the iteration count i and the length of the spatial series N, the discrepancy of the spectrum at i^{th} iteration was quantified as (Schreiber and Schmitz, 1996);

$$\text{Discrepancy} = \frac{\sum_{k=0}^{N-1} (\widehat{S}_k^{(i)} - \widehat{S}_k)^2}{\sum_{k=0}^{N-1} \widehat{S}_k^2}$$

2.2. Test of nonlinearity

The test of nonlinearity was performed by taking a statistical test for the original series and its surrogates. Among the various methods to test nonlinearity, third order autocovariance (C3), symmetry due to time reversibility (REV), and delay vector variance (DVV) are widely mentioned (Gautama et al., 2004; Jaksic et al., 2016; Schreiber and Schmitz, 1997). The third order autocovariance is a higher order extension of the traditional autocovariance and is given by $t^{C3}(\tau) = \langle x_k x_{k-\tau} x_{k-2\tau}\rangle$ (Schreiber and Schmitz, 1997). A time series is said to be reversible if its probabilistic properties are invariant with respect to the time reversal. A possible measure of the deviation for the asymmetry due to the time reversibility is given by $t^{REV}(\tau) = \langle (x_k - x_{k-\tau})^3\rangle$ where, τ is the time lag (Schreiber and Schmitz, 1997). A spatial series can be represented as a time series and the space lag can be represented as a time lag. Combining with a surrogate data strategy, both tests (C3 and REV) yield two tailed tests for nonlinearity. Whereas, the DVV method used in this manuscript obtained a single test statistic and the traditional (right-tailed) surrogate testing was performed. A comparison of these (C3, REV and DVV) methods is given by Gautama et al. (2004) using a set of synthetic time series with a gradually increasing degree of nonlinearity and the noise level and is beyond the scope of this manuscript. During the test, the null hypothesis was assumed that the series was driven by stationary, Gaussian processes. Among the methods, only DVV rejected the null hypothesis consistently for all the nonlinear series. The other methods failed to reject the linearity hypothesis one or more times even though the series contained certain degree of nonlinearity. Gautama et al. (2004) proved that the DVV method was superior over other commonly used methods as it yielded more consistent results than other methods and the results were straightforward to interpret. The DVV method also visualized the result in a DVV scatter diagram, which plotted the DVV curve against a globally linear model. A similar work by Jaksic et al. (2016) also proved the superiority of the method. Therefore, in our study, we used DVV to detect the nonlinearity in the spatial series of N_2O emissions from soil. The analysis was performed on the spatial series collected along a 128 point transect for 15 times to represent the 15 measurements over the study period.

DVV is a robust method that examined the predictability of a series in phase space at different scales. The method was based on the space delay embedding representation of a spatial series, $X = \{x(k), k = 1, \ldots, N\}$ where, N was a set of delay vectors (DVs) of a given embedding dimension m, which was given by $x(k) = [x_{k-m}, \ldots, x_{k-1}]$, a vector containing m (= 128) consecutive space samples. Every DV had a corresponding target. The steps of the analysis used in this work was summarized below (Gautama et al., 2004).

i. The DVs, $x(k) = [x_{k-m}, \ldots, x_{k-1}]$ and their corresponding targets $x_k$for a given embedding dimension, m (= 128) were generated.
ii. The mean, μ_d, and the standard deviation, σ_d, of all pair-wise distances between DVs, $\|x(i) - x(j)\|$ $(i \neq j)$ were computed.
iii. The sets Ω_k was generated in such a way that $\Omega_k = \{x(i), \|x(k) - x(i)\| \leq \tau_d\}$. This means the sets of all DVs that was closer to $x(k)$ than a certain distance, τ_d was taken from the interval $[min\{0, \mu_d - n_d\sigma_d\}, \mu_d + n_d\sigma_d]$, i.e. uniformly spaced, where, n_d was a parameter controlling the span over which the DVV analysis was performed.
iv. The variance of the corresponding targets, σ_k^2 for every set, Ω_k was computed.
v. The average over all sets, $\Omega_k$was calculated and normalized by the variance of the series, σ_x^2. This provided the measure of unpredictability, σ^{*2}: $\sigma^{*2} = \frac{(1/N)\sum_{k=1}^{N} \sigma_k^2}{\sigma_x^2}$. The variance measurement was considered valid, if the set, Ω_k contained at least 30 DVs.

The standardization of the distance axis made the DVV plots easy to interpret. The minimal target variance, i.e. the lowest point of the curve, was a measure for noise that was present in the series. The presence of a strong deterministic component led to small target variance for small spans.

In explaining the results, the DVV plots smoothly converged to unity at the extreme right. This was because for the maximum span, all DVs belonged to the same set and the variance of the target was equal to that of the series. In the next step, the DVV analysis was performed on both the original and the number of surrogate series to detect the linear and nonlinear nature present in them. The optimal embedding dimensions were used as in the original series. The standardization of the distance axis helped to combine the plots in a scatter diagram. The horizontal axis of the diagram corresponded to the DVV plot of the original series and the vertical axis corresponded to that of the surrogate series. If the surrogate series yielded DVV plots like that of the original series, the DVV scatter diagram coincided with the bisector line (equivalent to 1:1 line), and the original series was identified to be linear. The deviation of the scatter diagram from the bisector line indicated the nonlinearity in the original series (Gautama et al., 2004).

3. Materials and methods

3.1. Field site and sampling design

A field experiment was conducted at the St. Denis National Wildlife Area (SDNWA) (52°12′ N latitude, 106°50′ W longitude), which is located approximately 40 km east of Saskatoon, Saskatchewan, Canada. The details of the study site can be found in Yates et al. (2006) and Yates et al. (2007). In brief, the soils of this area are mainly Dark Brown Chernozem developed from moderately fine to fine textured, moderately calcareous, clayey glacio-lacustrine deposits and modified glacial till (Acton and Ellis, 1978). The terrain of this area is hummocky with 10–15% slopes and climate is semi-arid with a mean annual air temperature at the Saskatoon airport of 2 °C, with a monthly mean of − 19 °C in January and 18 °C in July. The 90-year mean annual precipitation at Saskatoon is 360 mm of which 84 mm occurs in winter, mostly as snow.

In June 2003, a sampling transect, extending in the north-south

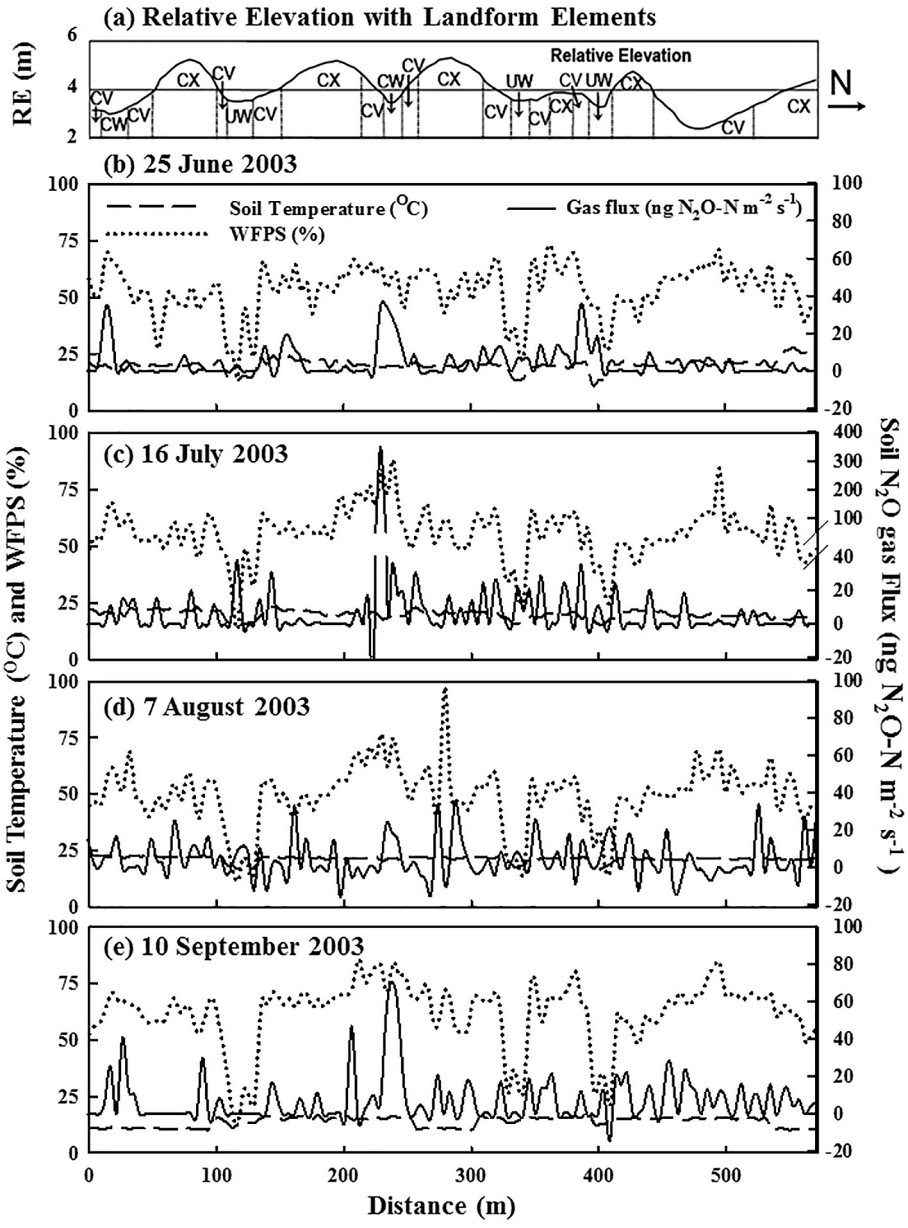

Fig. 1. Spatial distribution of a) relative elevation (RE, m) and landform elements, soil N_2O gas flux (ng N_2O-N m^{-2} s^{-1}), soil temperature (°C, 0–20 cm depth), and water filled pore space (WFPS, %, 0–15 cm depth) along the sampling transect on b) 25 June 2003, c) 16 July 2003, d) 7 September 2003 and e) 10 October 2003. Left side Y-axis shows the soil temperature and WFPS and right-side Y-axis shows the gas flux. Please note the change of scale and axis break on gas flux measurement on 16 July 2003 (c). The graph of relative elevation (a) shows different landform elements; CV stands for concave, CX stands for convex, UW stands for uncultivated wetlands and CW stands for cultivated wetlands.

direction, was established over several knolls and depressions representing different landform cycles (Fig. 1) after two years of fallow. The transect was 576 m long with 128 sampling points at 4.5 m equal intervals between points. In May 2004, the transect area, was seeded with mixed grass by Ducks Unlimited Canada. The topographic survey of this site was completed using a Sokkisha Set 5 Electronic Total Station (Sokkisha Co. Ltd. Tokyo, Japan) and a Trimble Pro XRS, Global Positioning System (Trimble Navigation, Sunnyvale, CA). The soil texture ranged from loam at topographically high positions to a silt loam at depressions. The bulk density was measured during laying out of the transect.

3.2. Soil nitrous oxide flux measurement

The N_2O flux was measured 15 times over the two-year period along the transect and the details can be found in Yates et al. (2006) and Yates et al. (2007). In brief, the N_2O emission was measured using a two-piece, closed vented chamber made of polyvinyl chloride. The gas samples were collected from the headspace of the chamber using a syringe and stored for laboratory analysis. Gas sampling was completed at three equally spaced time (t) intervals of 8 min with a separate time zero sample from each chamber. The four gas samples were taken from each chamber over a 24-min period at t_0, t_8, t_{16}, and t_{24}. Gas sample collection at each sampling day was completed in < 2 h time starting at midday.

N_2O concentrations were determined using a Varian CP3800 Gas Chromatograph (Varian Canada Inc., Mississauga, ON) equipped with dual electron capture detectors and Poraplot Q columns. The system was calibrated using standard gases (N_2O in N_2) obtained from PraxAir (Mississauga, ON). N_2O concentrations in the headspace samples were calculated from regression equations obtained by applying linear, least squares regression to the gas concentration (ppbV N_2O) versus peak area data. Samples of ambient air were included in each analytical run as reference to check the 'within run' precision, to calculate a minimum detectable concentration difference (MDCD), and to correct for detector drift (Yates et al., 2006). The MDCD was calculated by (i) analyzing matched paired of reference samples at regular interval during each analytical run, (ii) calculating the average difference between sample pairs, (μ_p) and the standard deviation, (σ_p) using the equation MDCD = $\mu_p + 2\sigma_p$. The MDCD was used to filter the raw data when

Table 1
Exploratory statistical test results of N_2O flux measurements along the transect at St. Denis National Wildlife Area during 2003 and 2004.

Measurement date	Mean	SD	CV	Max.	Min.	Skew.	Kurt.	Distribution shape
19-Jun-03	0.58	1.59	2.73	9.26	− 1.94	3.2	11.2	Semi-reverse J shaped
25-Jun-03	4.60	7.92	1.72	35.33	− 1.07	2.3	5.2	Reverse J shaped
7-Jul-03	21.56	40.20	1.86	354.47	0.00	5.8	41.0	Reverse J shaped
16-Jul-03	8.47	31.75	3.75	346.87	0.00	9.7	103.5	Reverse J shaped
7-Aug-03	4.53	10.03	2.21	34.44	− 15.71	1.0	1.0	Symmetrical
10-Sep-03	7.15	12.29	1.72	70.23	− 14.63	2.6	8.5	Semi-reverse J shaped
15-Oct-03	1.34	4.04	3.02	21.50	− 14.31	1.7	7.8	Symmetrical
30-Mar-04	2.33	4.80	2.06	22.26	− 7.76	1.8	5.2	Log normal
4-Apr-04	25.29	50.46	2.00	510.90	0.00	7.7	69.9	Reverse J shaped
29-Apr-04	17.34	92.66	5.34	876.08	− 8.19	7.7	64.0	Reverse J shaped
3-Jun-04	4.33	5.80	1.34	29.47	− 7.90	1.4	2.5	Log normal
23-Jun-04	− 0.18	1.90	− 10.85	5.17	− 10.23	− 2.1	10.3	Symmetrical
15-Jul-04	3.57	3.21	0.90	19.31	0.00	2.0	6.5	Log normal
18-Aug-04	0.24	1.79	7.50	8.96	− 4.41	2.4	9.3	Symmetrical
7-Oct-04	0.44	2.54	5.81	8.75	− 5.04	0.6	1.1	Symmetrical

*SD, Standard Deviation; CV, Coefficient of Variation; Max., Maximum; Min., Minimum; Skew., Skewness; Kurt. Kurtosis.

calculating the actual N_2O flux. If the sample concentration differences between each subsequent pair of time steps were all less than the MDCD, they were not considered to be significantly different from the t_0 concentration, and the flux was identified to be zero.

4. Results and discussions

4.1. Characteristics of gas emission data

The average emission fluxes were related to the probability distribution of fluxes measured along the transect. A lowest average emission of -0.18 ng N_2O-N m^{-2} s^{-1} was recorded on 23 June 2004, while the highest average emission of 25.29 ng N_2O-N m^{-2} s^{-1} was recorded on 4 April 2004 (Table 1). A very high average emission was also recorded on 7 July 2003, and 29 April 2003 (Table 1) but within the range reported from agricultural soils of the study region (Corre et al., 1996; Lemke et al., 1998; Pennock et al., 2005). Despite a medium average emission on 16 July 2003, the range of the measurement was very high. A similar high range in the flux measurements was also recorded on other dates (7 July 2003, 16 July 2003, 4 April 2008, 29 April 2008) leading to a data series with 'Reverse J' shaped statistical distributions (Table 1) (Yates et al., 2006). The non-normal statistical distributions mainly contributed from the highly variable spatial distribution of gas flux (Figs. 1 and 2). Fewer points with very large gas flux (e.g. 16 July 2003 (Fig.1), 4, April 2004 (Fig. 2)) made the gas flux highly skewed.

The highly skewed distribution of N_2O flux is very common and has been reported in other studies (Ambus and Christensen, 1994; Corre et al., 1996; Parkin, 1987). Brumme et al. (1999) proposed a relationship between the average N_2O flux and the type of distribution that existed in a dataset. The increase or decrease of the emissions is occasionally dictated by the extreme peak of the emission that is controlled by the climatic events such as drying/wetting, freezing/thawing, erratic behaviour of precipitation or the spring snowmelt. The measurements on 7 August 2003 (Fig. 1), 15 October 2003, 23 June 2004, 18 August 2004 (Fig. 2), and 7 October 2004 were recorded with a very low average emission (Table 1) and symmetrical data distribution. The data distribution of log normal and semi-reverse J shape was also recorded with a low to medium average emission. When the average flux decreased, the skewness of the distribution decreased and yielded a log normal distribution. With a further decrease in average flux, the distribution became symmetrical (Yates et al., 2006).

Yates et al. (2006) reported that the relationship between probability distributions of N_2O flux and the average flux was a product of the control from landform positions and land uses along the transect. During the early spring, large fluxes were concentrated on convex landform elements which were mainly free of snow cover and exhibited high soil moisture (Figs. 1 and 2). With time, the snowmelt water concentrated at the depressions including the cultivated and uncultivated wetlands. Often the standing water in these wetlands facilitated the denitrification processes leading to high emissions that skewed the data severely and changed the distribution from log normal to reverse J shaped (Nieder and Benbi, 2008; Yates et al., 2006). The topographic elements (Figs. 1 and 2) controlled the distribution of water in the landscape and thus, the water filled pore space (WFPS) in soil and the gas emission processes. The soil temperature was also controlled by the topographic elements and thus, controlled the flux (Figs. 1 and 2) (Groffman and Tiedje, 1989; Tian et al., 2015; Yates et al., 2007).

4.2. Detecting nonlinearity in the spatial series of N_2O flux

4.2.1. Determination of optical parameters of DVV

An optimized value for embedding dimension, $m = 2$ and space delay, $\tau = 1$ (Fig. 3) were identified for the total of 15 spatial series of N_2O fluxes using the differential entropy method (Gautama et al., 2003). Selection of these embedding parameters are central to the chaotic dynamical system and are critical for the detection of nonlinearity. The optimal set of parameters (m, τ) yielded a phase-space representation that best reflected the dynamics of the soil system and the processes associated with gas fluxes.

4.2.2. Presence of linearity/nonlinearity in the spatial series of N_2O flux over the whole period

A set of 99 surrogates were created using the IAAFT method and used along with optimized embedding parameters to calculate the delay vectors for all the datasets of N_2O flux measurements. The DVV scatter diagrams indicated that the spatial series of N_2O emissions on 19 June 2003, 16 July 2003, 10 September 2003, 15 October 2003, 30 March 2004, 4 April 2004, 29 April 2004, 3 June 2004 and 7 October 2004 were deviated from the bisector line suggesting the presence of nonlinearity (Fig. 4). Deviation from the bisector line indicated that the DVV plot of the original series was different from that of the surrogates. As we used the optimal embedding function of the original series, the probability density function and the power spectrum of the surrogates were the same as the original series but with different distributions (Gautama et al., 2004). Thus, a 1:1 relationship (bisector line) between DVV plots indicated the presence of linearity (destruction of the distribution during surrogate generation) while the deviation indicated the presence of nonlinearity in the original spatial series. The remaining 10 spatial series of N_2O measurements were linear in nature (Table 2). The presence of linearity/nonlinearity in the N_2O flux measurement series

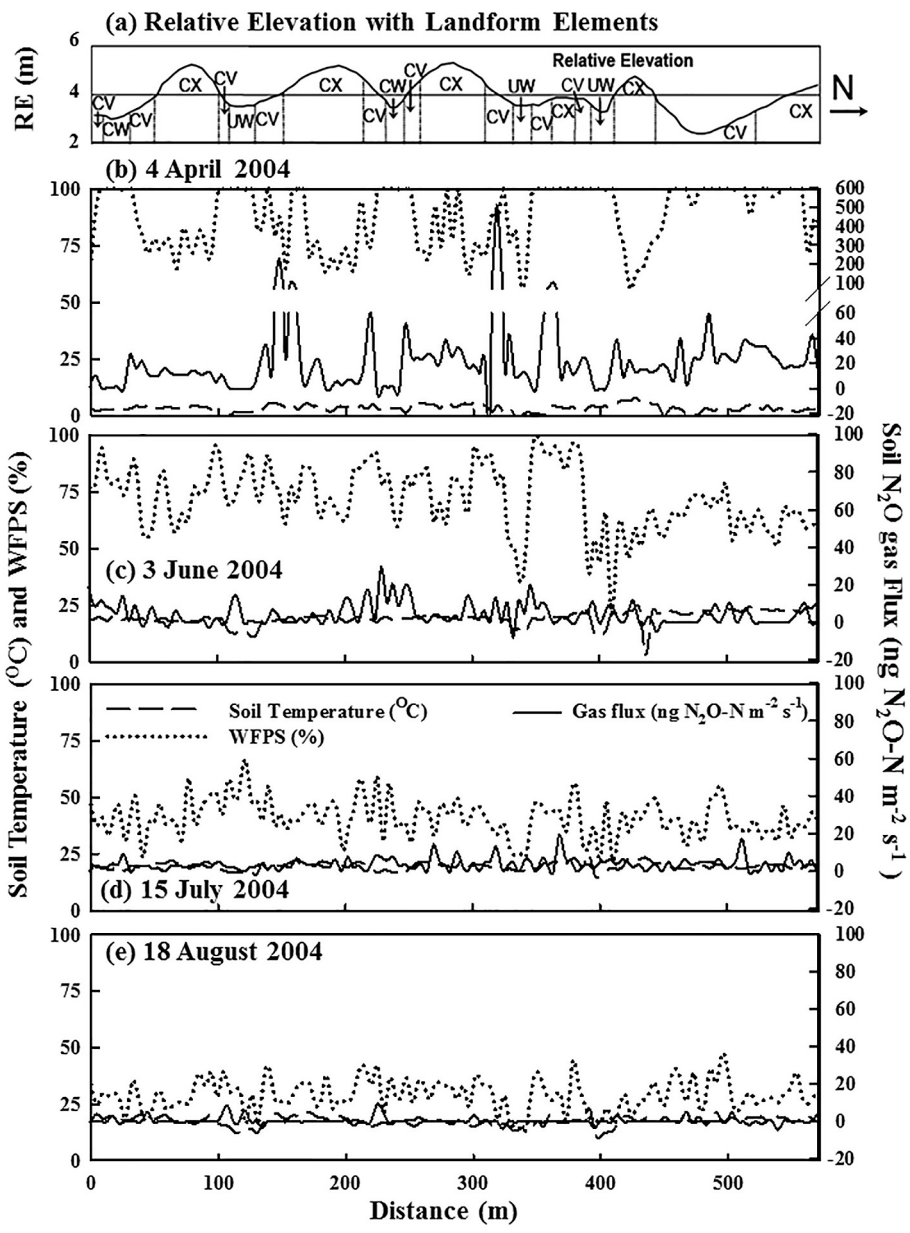

Fig. 2. Spatial distribution of a) relative elevation (RE, m) and landform elements, soil N_2O gas flux (ng N_2O-N m^{-2} s^{-1}), soil temperature (°C, 0–20 cm depth), and water filled pore space (WFPS, %, 0–15 cm depth) along the sampling transect on b) 4 April 2004, c) 3 June 2004, d) 15 July 2004 and e) 18 August 2004. Left side Y-axis shows the soil temperature and WFPS and right-side Y-axis shows the gas flux. Please note the change of scale and axis break on gas flux measurement on 4 April 2004 (b). The graph of relative elevation (a) shows different landform elements; CV stands for concave, CX stands for convex, UW stands for uncultivated wetlands and CW stands for cultivated wetlands.

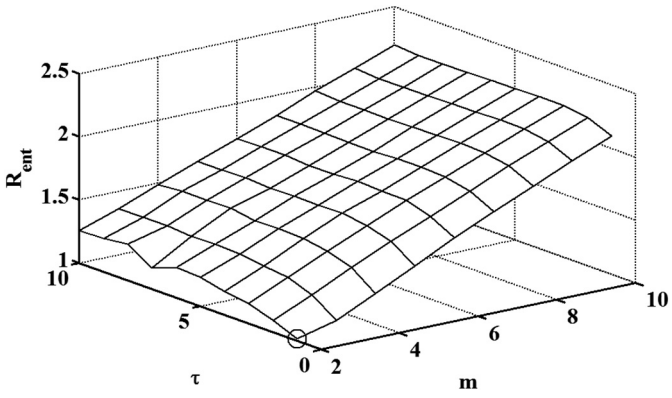

Fig. 3. Optimized value for embedding dimension, m and time/space delay, τ for the total of 15 spatial series of N_2O measurements using the differential entropy method.

was also confirmed from the DVV rank test performed at a significance level of 0.1. A total of nine out of the fifteen measurement times, the spatial series of fluxes were detected with nonlinearity. The variable nature of the presence of linearity/nonlinearity along the transect over the measurement times might have developed from the underlying dominant soil processes and other controlling factors.

4.2.3. Presence of linearity/nonlinearity during the early spring/spring

The flux measured from the early spring (late-March) to the early summer (mid-June) (i.e. 19 June 2003, 30 March 2004, 4 April 2004, 29 April 2004, 3 June 2004) exhibited nonlinearity with a rank test value > 0.9 (Table 2). This indicated that the DVVs were significantly different from the bisector line (Fig. 4) and the presence of nonlinearity in the spatial series of those measurement dates. In the study area, generally the snow started to melt during late-March and continued until the mid- to late-April. Drifting snow from the strong winds of the Prairie and the uneven distribution of snowmelt water in the hummocky landscape created a unique set of hydrological problems (Biswas and Si, 2011; Flerchinger and Cooley, 2000). Small amounts of snow on the knolls started to melt first creating snow free ground with high soil water content. The flux on 30 March 2004 (Fig. 2) was completed during the peak period of snowmelt with uneven distribution of snow cover including the knolls with no snow and depressions with thick

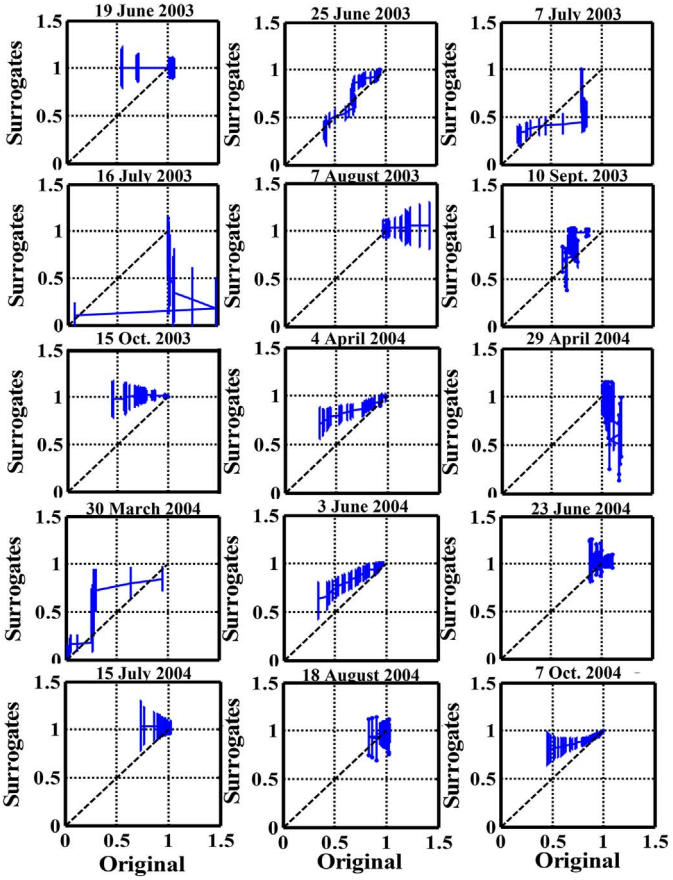

Fig. 4. Scatter plots of the delay vector variance for the measured N_2O series (X-axis) and the surrogates (Y-axis). The bisector line was represented by dashed line and the delay vectors with error bar were presented by points connected with solid line.

Table 2
The DVV rank results for linearity/nonlinearity of 15 N_2O flux measurements.

Date	DVV	Results
19-Jun-03	0.95	Nonlinear
25-Jun-03	0.80	Linear
7-Jul-03	0.82	Linear
16-Jul-03	0.97	Nonlinear
7-Aug-03	0.81	Linear
10-Sep-03	0.99	Nonlinear
15-Oct-03	0.99	Nonlinear
30-Mar-04	0.97	Nonlinear
4-Apr-04	0.95	Nonlinear
29-Apr-04	0.94	Nonlinear
3-Jun-04	0.95	Nonlinear
23-Jun-04	0.27	Linear
15-Jul-04	0.68	Linear
18-Aug-04	0.12	Linear
7-Oct-04	0.98	Nonlinear

snow cover. The infiltration of snowmelt water on the knoll created a favourable situation for denitrifying bacterial activity. Additionally, the snow-free ground exhibited a slightly higher temperature than other locations and contributed to the denitrification processes (Fig. 2). The localized elevated denitrification process created hotspots or the intermittency for N_2O emissions from soil (Figs. 1 and 2). Lark et al. (2004a) reported the intermittency in the rate of N_2O emissions from soil along a transect from an arable land at Silsoe in England. This was markedly controlled by the non-linear processes, as the denitrification takes place only when the water present in soil is above a threshold level (Webster and Goulding, 1989). The intermittency indicated that the emission did not follow a regular pattern, meaning the output of the soil system or the N_2O emissions from soil was not linearly proportional to the factors controlling it across the entire range of controls or the input variables (McSwiney and Robertson, 2005; Phillips, 2003; Shcherbak et al., 2014). With time, as the snow melted along the slope (during May), the N_2O emission hotspots have also shifted along the slopes (Figs. 1 and 2). The depressions received a lot of water from the surrounding snow melts, resulting in elevated soil water content and created a favourable condition for denitrification processes. The nonlinear nature of the underlying processes of gas emission such as denitrification resulted in nonlinearity in the flux measurements. Generally, at the end of May to the middle of June, depressions started to lose the standing water with the growth of plants. However, the evapotranspiration processes were not very prominent over the field due to the young age of the vegetation. Thus, the hotspots for denitrification were depression-focused creating the nonlinearity in the flux measurements (Figs. 1 and 2).

4.2.4. Presence of linearity/nonlinearity during the growing season

The spatial series of flux measured during the peak growing period (25 June 2003, 7 July 2003, 7 August 2003, 23 June 2004, 15 July 2004, 18 August 2004) exhibited linearity (Table 2). The DVV scatter diagram did not show deviation from the bisector line (Fig. 4). There was an exception for the flux measured on 16 July 2003, which was detected with nonlinearity. Once the grasses were established in the field, evapotranspiration demand was the major process controlling the soil water dynamics. In general, grasses grew better in depressions (growing densely and up to 2-m tall) than on knolls, where soil stored little water compared to depressions. The extra water in the depression allowed plants to withdraw more water and grow vigorously. The depressions lost more water when compared to knolls, thereby, decreasing the range of the soil water stored at different landscape positions (Biswas, 2014; Biswas et al., 2012). In this situation, evapotranspiration process generally ruled over other processes to control the soil water status and thus, the processes of N_2O emissions from soil. This linear relationship is also reflected in the flux measurements (McSwiney and Robertson, 2005; Shcherbak et al., 2014).

4.2.5. Presence of linearity/nonlinearity during the fall

The spatial series of flux measured (Figs. 1 and 2) during the fall to late fall (10 September 2003, 15 October 2003, and 7 October 2004) was also detected with nonlinearity. The microbial activity during this period generally approached at its peak. The favourable water content and soil temperature led to the nitrification processes over denitrification and were mainly responsible for the emission of N_2O from soil (Shcherbak et al., 2014; Skiba et al., 1993; Tian et al., 2015; Tiedje, 1988). However, the amount of N_2O that nitrification process can contribute was generally lower than the denitrification processes. During the fall or at the end of the growing season, the variability in water content was mainly dictated by the landform elements as the evapotranspiration processes slowed down with the maturity of crops/grasses. Despite the small amount, the water stored in soil was variable leading to differences in the underlying processes controlling the flux and making the spatial series nonlinear (Figs. 1 and 2).

4.2.6. Presence of linearity/nonlinearity and its relationship with other factors

The heterogeneity in the N_2O emissions from soil was modified by the variability of different processes including denitrification and nitrification (Creze, 2015; Shcherbak et al., 2014; Skiba et al., 1993; Tiedje, 1988). A suite of environmental factors including topographic elements, water content of soil and the soil properties that controlled the N_2O emission processes (Figs. 1 and 2) (Ambus and Christensen, 1994; McSwiney and Robertson, 2005; Shcherbak et al., 2014; Tian et al., 2015; Tiedje, 1988; Yates et al., 2006). Topography elements were considered as the basic factors controlling the gas emission processes by regulating the hydrology in this type of landscape. Generally,

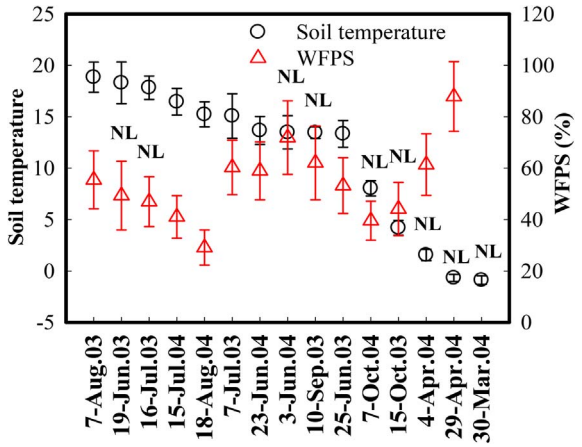

Fig. 5. Average water filled pore space (0–15 cm depth) and soil temperature (0–20 cm depth) along the transect for the measurement dates during 2003 and 2004. Error bars indicated standard deviation. Water filled pore space was absent for 30 march 2004 due to frozen soil. Data are presented in the order of increasing means of soil temperature. NL indicated nonlinearity and was used to mark the dates exhibited nonlinearity in the spatial series.

the topographic elements controlled the snow melt processes and redistributed the soil water and energy in the soil surface, especially after snowmelt and rainfall events (Corre et al., 1996; Nishina et al., 2009; Yates et al., 2006). The WFPS and the soil temperature (Figs. 1 and 2) also controlled the denitrification and nitrification processes and thus, the flux (Lemke et al., 1998; Nishina et al., 2009). The presence of nonlinearity in the N_2O flux with different WFPS and temperature was presented in Fig. 5. In general, nonlinearity was detected in the N_2O fluxes with low surface soil (0–20 cm) temperatures (15 October 2003, 30 March 2004, 4 April 2004, 29 April 2004, and 7 October 2004). Sometime, the low temperature was accompanied by high WFPS (15 October 2003, 4 April 2004, and 29 April 2004) (Fig. 5). However, no distinct relationships were observed among soil temperature, WFPS and the presence of nonlinearity. More detailed future work is necessary to understand the relationship between WFPS, temperature and the presence of nonlinearity in the spatial series of N_2O emission from soil to develop, test and validate different environmental models.

Overall, the DVV method detected nonlinearity in the spatial series of N_2O flux from soil. The variations in the spatial series with nonlinearity was related to the variations in underlying factors and processes. Though the majority of the methods used to identify nonlinearity in the time series with substantial data, DVV showed a consistent and moderately robust performance in detecting nonlinearity in a spatial series with a small number of measurements, which is often the case for spatial series of soil properties. This is particularly true for properties that are difficult to measure in field conditions, such as N_2O flux. The information on the presence of nonlinearity in the spatial series of N_2O flux will be the guide for choosing the methods for spatial variability quantification.

5. Conclusion

In this study, the delay vector variance method was used to detect the nonlinearity associated with N_2O flux in the hummocky landscape of central Canada. More than 60% of the N_2O flux measurements completed at different sampling times over a two-year period were associated with nonlinearity. The spatial series of the measurements carried out during the early spring to spring and the fall season exhibited nonlinearity. The water content in soil as controlled by topography was a major factor in determining the soil processes including denitrification and nitrification, which in turn controlled the emission of N_2O gases from soil. The nonlinearity in N_2O emissions was detected with low soil temperature and high water filed pore spaces but without any definite relationship. Thus, the delay vector variance method showed promise in detecting nonlinearity in soil or in environmental variables.

Acknowledgements

The dataset was collected by Dr. Tom Yates and his team. We greatly appreciate their support for the data collection, measurement and processing. This work was supported financially by the Natural Science and Engineering Research Council (NSERC) of Canada (RGPIN-2014-4100) (NSERC Discovery of Dr. Asim Biswas), the National Natural Science Foundation of China (41571219, 41371296) and Young Scientist's Group of China (DLSXZ1605).

References

Acton, D.F., Ellis, J.G., 1978. The soils of Saskatoon Map area 73B Saskatchewan. In: Saskatchewan Institute of Pedology Publication S4. University of Saskatchewan, Saskatoon, SK, Canada.
Ambus, P., Christensen, S., 1994. Measurement of N_2O emission from a fertilized grassland - an analysis of spatial variability. J. Geophys. Res.-Atmos. 99 (D8), 16549–16555.
Anthony, W.H., Hutchinson, G.L., Livingston, G.P., 1995. Chamber measurement of soil-atmosphere gas exchange: linear vs. diffusion-based flux models. Soil Sci. Soc. Am. J. 59 (5), 1308–1310.
Biswas, A., 2014. Landscape characteristics influence the spatial pattern of soil water storage: similarity over times and at depths. Catena 116 (0), 68–77.
Biswas, A., Si, B.C., 2011. Identifying scale specific controls of soil water storage in a hummocky landscape using wavelet coherency. Geoderma 165 (1), 50–59.
Biswas, A., Si, B.C., 2013. Scale dependence and time stability of nonstationary soil water storage in a hummocky landscape using global wavelet coherency. In: Grundus, S., Stępniewski, A. (Eds.), Advances in Agrophysical Research. InTech, pp. 97–114.
Biswas, A., Chau, H.W., Bedard-Haughn, A.K., Si, B.C., 2012. Factors controlling soil water storage in the hummocky landscape of the Prairie Pothole Region of North America. Can. J. Soil Sci. 92 (4), 649–663.
Biswas, A., Cresswell, H.P., Viscarra Rossel, R.A., Si, B.C., 2013. Characterizing scale- and location-specific variation in non-linear soil systems using the wavelet transform. Eur. J. Soil Sci. 64 (5), 706–715.
Brumme, R., Borken, W., Finke, S., 1999. Hierarchical control on nitrous oxide emission in forest ecosystems. Glob. Biogeochem. Cycles 13 (4), 1137–1148.
Casdagli, M., 1992. Chaos and deterministic versus stochastic non-linear modelling. J. R. Stat. Soc. Ser. B Methodol. 54 (2), 303–328.
Corre, M.D., vanKessel, C., Pennock, D.J., 1996. Landscape and seasonal patterns of nitrous oxide emissions in a semiarid region. Soil Sci. Soc. Am. J. 60 (6), 1806–1815.
Corwin, D.L., Hopmans, J., de Rooij, G.H., 2006. From field- to landscape-scale vadose zone processes: scale issues, modeling, and monitoring. Vadose Zone J. 5 (1), 129–139.
Creze, C., 2015. Greenhouse Gas Emissions from an Intensively Cropped Field under Various Water and Fertilizer Management Practices. McGill University, Montreal, Canada.
Culling, W.E.H., 1988. Dimension and entropy in the soil-covered landscape. Earth Surf. Process. Landf. 13 (7), 619–648.
Emanuel, G., 1997. Nonlinear systems: between a law and a definition. Rep. Prog. Phys. 60 (10), 1063.
Environment Canada, 2008. Canada's Greenhouse Gas Emissions: Understanding the Trends, 1990–2006. Environment Canada, Ottawa.
Flerchinger, G.N., Cooley, K.R., 2000. A ten-year water balance of a mountainous semi-arid watershed. J. Hydrol. 237 (1–2), 86–99.
Fuchs, A., 2013. Nonlinear Dynamics in Complex Systems. Springer Berlin Heidelberg, Berlin.
Gautama, T., Mandic, D.P., Hulle, M.M.V., 2003. A differential entropy based method for determining the optimal embedding parameters of a signal, acoustics, speech, and signal processing, 2003. In: Proceedings. (ICASSP '03). 2003 IEEE International Conference on. Vol. 26 (pp. VI-29-32).
Gautama, T., Mandic, D.P., Van Hulle, M.A., 2004. The delay vector variance method for detecting determinism and nonlinearity in time series. Physica D 190 (3–4), 167–176.
Groffman, P.M., Tiedje, J.M., 1989. Denitrification in north temperate forest soils: spatial and temporal patterns at the landscape and seasonal scales. Soil Biol. Biochem. 21 (5), 613–620.
Heuvelink, G.B.M., Pebesma, E.J., 1999. Spatial aggregation and soil process modelling. Geoderma 89 (1–2), 47–65.
IPCC, 2007. Contribution of Working Group III to the Fourth Assessment Report of the Intergovernmental Panel on Climate Change, 2007, Intergovernmental Panel on Climate Change. NY, USA, New York.
Jaksic, V., Wright, C., Mandic, D.P., Murphy, J., Pakrashi, V., 2015. A delay vector variance based marker for an output-only assessment of structural changes in tension leg platforms. J. Phys. Conf. Ser. 628 (1), 012059.
Jaksic, V., Mandic, D.P., Ryan, K., Basu, B., Pakrashi, V., 2016. A comprehensive study of the delay vector variance method for quantification of nonlinearity in dynamical systems. R. Soc. Open Sci. 3 (1).
Kachanoski, R.G., Rolston, D.E., Dejong, E., 1985. Spatial and spectral relationships of soil

properties and microtopography. 1. Density and thickness of A-horizon. Soil Sci. Soc. Am. J. 49 (4), 804–812.
Kaplan, D.T., 1994. Exceptional events as evidence for determinism. Physica D 73 (1–2), 38–48.
Kroon, P.S., Hensen, A., van den Bulk, W.C.M., Jongejan, P.A.C., Vermeulen, A.T., 2008. The importance of reducing the systematic error due to non-linearity in N_2O flux measurements by static chambers. Nutr. Cycl. Agroecosyst. 82 (2), 175–186.
Lark, R.M., Milne, A.E., Addiscott, T.M., Goulding, K.W.T., Webster, C.P., O'Flaherty, S., 2004a. Analysing spatially intermittent variation of nitrous oxide emissions from soil with wavelets and the implications for sampling. Eur. J. Soil Sci. 55 (3), 601–610.
Lark, R.M., Milne, A.E., Addiscott, T.M., Goulding, K.W.T., Webster, C.P., O'Flaherty, S., 2004b. Scale- and location-dependent correlation of nitrous oxide emissions with soil properties: an analysis using wavelets. Eur. J. Soil Sci. 55 (3), 611–627.
Lemke, R.L., Izaurralde, R.C., Nyborg, M., 1998. Seasonal distribution of nitrous oxide emissions from soils in the Parkland region. Soil Sci. Soc. Am. J. 62 (5), 1320–1326.
Mandic, D.P., Chen, M., Gautama, T., Van Hulle, M.M., Constantinides, A., 2008. On the characterization of the deterministic/stochastic and linear/nonlinear nature of time series. Proc. R. Soc. London, A Science 464 (2093), 1141–1160.
McSwiney, C.P., Robertson, G.P., 2005. Nonlinear response of N2O flux to incremental fertilizer addition in a continuous maize (*Zea mays* L.) cropping system. Glob. Chang. Biol. 11 (10), 1712–1719.
Millan, H., Garcia-Fornaris, I., Gonzalez-Posada, M., 2009. Nonlinear spatial series analysis from unidirectional transects of soil physical properties. Catena 77 (1), 56–64.
Milne, A.E., Haskard, K.A., Webster, C.P., Truan, I.A., Goulding, K.W.T., Lark, R.M., 2011. Wavelet analysis of the correlations between soil properties and potential nitrous oxide emission at farm and landscape scales. Eur. J. Soil Sci. 62 (3), 467–478.
Milne, A.E., Haskard, K.A., Webster, C.P., Truan, I.A., Goulding, K.W.T., Lark, R.M., 2013. Wavelet analysis of the variability of nitrous oxide emissions from soil at decameter to kilometer scales. J. Environ. Qual. 42 (4), 1070–1079.
Nieder, R., Benbi, D.K., 2008. Carbon and Nitrogen in the Terrestrial Environment, 1 ed. Springer Netherlands, The Nethorlands.
Nishina, K., Takenaka, C., Ishizuka, S., 2009. Spatial variations in nitrous oxide and nitric oxide emission potential on a slope of Japanese cedar (*Cryptomeria japonica*) forest. Soil Sci. Plant Nutr. 55 (1), 179–189.
Pai, P.F., Palazotto, A.N., 2008. Detection and identification of nonlinearities by amplitude and frequency modulation analysis. Mech. Syst. Signal Process. 22 (5), 1107–1132.
Parkin, T.B., 1987. Soil microsites as a source of denitrification variability1. Soil Sci. Soc. Am. J. 51 (5), 1194–1199.
Pennock, D., Farrell, R., Desjardins, R., Pattey, E., MacPherson, J.I., 2005. Upscaling chamber-based measurements of N_2O emissions at snowmelt. Can. J. Soil Sci. 85 (1), 113–125.
Phillips, J.D., 1998. On the relations between complex systems and the factorial model of soil formation (with discussion). Geoderma 86 (1–2), 1–21.
Phillips, J.D., 2003. Sources of nonlinearity and complexity in geomorphic systems. Prog. Phys. Geogr. 27 (1), 1–23.
Phillips, J.D., 2008. Soil system modelling and generation of field hypotheses. Geoderma 145 (3–4), 419–425.
Schreiber, T., 1999. Interdisciplinary application of nonlinear time series methods. Phys. Rep. 308 (1), 1–64.
Schreiber, T., Schmitz, A., 1996. Improved surrogate data for nonlinearity tests. Phys. Rev. Lett. 77 (4), 635–638.
Schreiber, T., Schmitz, A., 1997. Discrimination power of measures for nonlinearity in a time series. Phys. Rev. E 55 (5), 5443–5447.
Schreiber, T., Schmitz, A., 2000. Surrogate time series. Physica D 142 (3–4), 346–382.
Shcherbak, I., Millar, N., Robertson, G.P., 2014. Global metaanalysis of the nonlinear response of soil nitrous oxide (N_2O) emissions to fertilizer nitrogen. Proc. Natl. Acad. Sci. 111 (25), 9199–9204.
Si, B.C., 2008. Spatial scaling analyses of soil physical properties: a review of spectral and wavelet methods. Vadose Zone J. 7 (2), 547–562.
Skiba, U., Smith, K.A., fowler, D., 1993. Nitrification and denitrification as sources of nitric oxide and nitrous oxide in a sandy loam soil. Soil Biol. Biochem. 25 (11), 1527–1536.
Theiler, J., Eubank, S., Longtin, A., Galdrikian, B., Doyne Farmer, J., 1992. Testing for nonlinearity in time series: the method of surrogate data. Physica D 58 (1), 77–94.
Tian, H., Chen, G., Lu, C., Xu, X., Ren, W., Zhang, B., Banger, K., Tao, B., Pan, S., Liu, M., Zhang, C., Bruhwiler, L., Wofsy, S., 2015. Global methane and nitrous oxide emissions from terrestrial ecosystems due to multiple environmental changes. Ecosyst. Health Sustain. 1 (1), 1–20.
Tiedje, J.M., 1988. Ecology of denitrification and dissimilatory nitrate reduction to ammonium. In: Biology of Anaerobic Microorganisms. 717. pp. 179–244.
Trangmar, B.B., Yost, R.S., Uehaa, G., 1985. Application of geostatistics to spatial studies of soil properties. Adv. Agron. 38, 45–94.
Turchin, P., Taylor, A.D., 1992. Complex dynamics in ecological time-series. Ecology 73 (1), 289–305.
Webster, C.P., Goulding, K.W.T., 1989. Influence of soil carbon content on denitrification from fallow land during autumn. J. Sci. Food Agric. 49 (2), 131–142.
Yates, T.T., Si, B.C., Farrell, R.E., Pennock, D.J., 2006. Wavelet spectra of nitrous oxide emission from hummocky terrain during spring snowmelt. Soil Sci. Soc. Am. J. 70 (4), 1110–1120.
Yates, T.T., Si, B.C., Farrell, R.E., Pennock, D.J., 2007. Time, location, and scale dependence of soil nitrous oxide emissions, soil water, and temperature using wavelets, cross-wavelets, and wavelet coherency analysis. J. Geophys. Res.-Atmos. 112 (D9). http://dx.doi.org/10.1029/2006JD007662.